Electronic Supplementary Material (ESI) for Physical Chemistry Chemical Physics.

Isolating the Spectral Signature of H_3O^+ in the Smallest Droplet of Dissociated HCl Acid

John S. Mancini, Joel M. Bowman*

Cherry L. Emerson Center for Scientific Computation and,
Department of Chemistry, Emory University, Atlanta, GA 30322

*To whom correspondence should be addressed; E-mail: jmbowma@emory.edu.

1 Details of LMon Potential Energy Surface

The newly developed LMon PES considered all one- two- and three-body H_3O^+ interactions. The contribution of each of interaction terms in the SIP are given in Table 1. The details of each of the interaction potentials included in the LMon PES are shown in Table 2. The $H_3O^+H_2O$ interaction energy and dipole moment were taken as the intrinsic interaction energy and dipole moments of a previously reported PES and DMS. (S*1*) All other interactions were taken from fits to a 5th order permutationally invariant polynomial with a basis of Morse like variables, $exp(-r_{ij}/\lambda)$, where r_{ij} are the intermolecular distances and the range parameter, λ, equals 2 bohr. (S*2*) Explicitly the two- and three-body interactions are computed using the following two equations where the indices, i, j, and k refer to monomer units.

$$V_{\text{two-body}}(i,j) = V_{\text{dimer}}(i,j) - (V_{\text{monomer}}(i) + V_{\text{monomer}}(j)) \tag{1}$$

$$\begin{aligned} V_{\text{three-body}}(i,j,k) = V_{\text{trimer}}(i,j,k) - (V_{\text{dimer}}(i,j) + V_{\text{dimer}}(i,k) + V_{\text{dimer}}(k,j)) \\ -3(V_{\text{monomer}}(i) + V_{\text{monomer}}(j) + V_{\text{monomer}}(k)) \end{aligned} \tag{2}$$

For a given interaction, the same level of theory was used to compute all of the required monomer, dimer and trimer energies. The points for the new potentials were taken from sections of the geometries which are sampled in the MULTIMODE calculations. More specifically, the points are the displacements of one-, two-, three- and four-mode grids of the LMon modes of the CCSD(T)-F12a/aVDZ configuration. The fitting was done in an iterative fashion whereby addition points were added to the fitting data base until no significant changes were observed in the harmonic and anharmonic frequencies with respect to the addition of more points. The potentials were also tested using classical molecular dynamics and Diffusion Monte Carlo simulations of the embedded H_3O^+. The LMon DMS was formulated in a similar manner and contains all one- and two-body H_3O^+ dipole interactions computed using MP2/aVTZ. The details of each of the LMon DMS parts are shown in Table 3 These and all other reported *ab initio* calculations were performed using the electronic structure package MOLPRO 2010. (S*3*)

2 Analysis of H_3O^+ Harmonic Frequencies and the Structure in the SIP Configuration

A geometry optimization of the SIP cluster was performed using MP2/aVDZ and its full H_3O^+ harmonic frequencies were computed; these values are reported in Table 4. Table 6 summarizes the previously reported values of the SIP H_3O^+ harmonic frequencies computed at different levels of theory. A comparison of the H_3O^+ embedded structure parameters for the CCSD(T)-F12/aVDZ and LMon PES optimized structures are provided in Table 5.

3 MULTIMODE Calculation Details

The MULTIMODE basis was limited to those states having a total number of quantum less than or equal to eight with a maximum of eight quanta allowed in each modes. Each mode used ten

G. Hermite integration points.

The twelve-mode MULTIMODE calculation reported in the main text included four-mode coupling, that is to say the potential was represented in terms of a maximum of four varying modes. Changes in peak positions and intensities were progressively smaller moving from two- to three- and then four-mode coupling, indicating our calculations had converged or were close to convergence. Due to the exponential increase in computation time, calculations involving five-mode or greater coupling could not be performed in a reasonable amount of time to further verify that twelve mode calculation was converged. Further support for the convergence is provided in by the results of a reduced dimensional calculations involving only the six highest frequency modes where five-mode coupled calculations were performed. The peak positions in these reduced dimensional calculations changed by less than 1 cm^{-1} when increased from four- to five-mode coupling.

In the MULTIMODE spectrum each VCI state is characterized by a set of optimized virtual VSCF state coefficients. In vibrational calculations with a small level of mode mixing VCI states are characterized by predominately one VSCF state with the square of the its respective coefficient equaling between 0.8 and 0.9 (where 1.0 would indicate completely pure state). In the present study, the VCI states reported for calculations of the H_3O^+ are highly mixed. These VCI states are characterized by dominate squared coefficients equaling less 0.5. Due to the heavy state mixing and the large (206) number of observed IR active states, we adopted a method to characterize the convoluted Gaussian bands of the spectra based on the contribution of virtual VSCF states in the band. We first identified the ranges of each Gaussian peak whose intensities were greater than 10% of the most intense Gaussian peak. The coefficients of the each VCI states in the Gaussian peak were squared, scaled by the VCI state's intensity and then summed over all VCI states. The analysis gives a qualitative picture of the contribution of each independent VSCF virtual state over the range of several VCI states which from Gaussian

peaks. The results of this analysis for VSCF virtual which contribute at least 50% of the largest virtual state coefficients are shown in Table 7 for the eight reported peaks. We note in the case of the asymmetric stretch peak the sum of the two degenerate VCI states has the largest contribution in the associated band.

4 Unionized $HCl(H_2O)_4$ and the Higher Energy Form of the SIP Configuration

Figure 1 contains a representation of the higher energy, $\sim$200 cm^{-1}, non-symmetric SIP configuration and representations of the three forms of the unionized $HCl(H_2O)_4$ clusters. Full harmonic frequencies for the non-symmetric SIP configuration computed using MP2/aVDZ are reported in Table 8. Higher quality CCSD(T)-F12/aVDZ LMon harmonic frequencies are reported in Table 9.

References

S1. X. Huang, B. J. Braams, J. M. Bowman, *J. Chem. Phys.* **122**, 44308 (2005).

S2. B. J. Braams, J. M. Bowman, *Int. Rev. in Phys. Chem.* **28**, 577 (2009).

S3. Werner, h.-j.; knowles, p. j.; knizia, g.; et al. molpro, version 2010.1, a package of ab initio programs. http://www.molpro. net (2010).

S4. S. Re, Y. Osamura, Y. Suzuki, H. F. Schaefer, *J. Chem. Phys.* **109**, 973 (1998).

S5. D. E. Bacelo, R. C. Binning, Y. Ishikawa, *J. Phys. Chem. A* **103**, 4631 (1999).

S6. A. Gutberlet, *et al.*, *Science* **324**, 1545 (2009).

S7. S. D. Flynn, *et al.*, *J. Phys. Chem. Lett.* **1**, 2233 (2010).

S8. M. Letzner, *et al.*, *J. Chem. Phys.* **139**, 154304 (2013).

Table 1: Details of the SIP many-body interactions from CCSD(T)-F12/aVDZ.

Interaction	kcal	|Percentage|
$(H_3O)Cl$	-111.0	43.0
$H_3O(H_2O)$	-80.8	31.3
$(H_2O)Cl$	-39.6	15.4
$H_3O(H_2O)_2$	15.6	6.0
$(H_2O)_2Cl$	4.7	1.8
$(H_2O)_2$	2.7	1.1
$H_3O(H_2O)Cl$	1.7	0.7
4-body + 5-body	-1.5	0.6
$(H_2O)_3$	-0.4	0.1

Table 2: Details of the components of the PES surface's total number of points, fitting root-mean-squared-deviation (RMSD) and energy span.

Interaction	H_3O^+	$H_3O^+Cl^-$	$H_3O^+H_2O$	$H_3O^+(H_2O)Cl^-$	$H_3O^+(H_2O)_2$
Method	CCSD(T)-F12b/aVQZ	CCSD(T)-F12b/aVTZ	CCSD(T)/aVTZ	CCSD(T)-F12b/aVDZ	CCSD(T)-F12b/aVTZ
Total Points	1601	11307	48189	28073	21740
RMSD (cm^{-1})	9	10	35	9	6
Energy Span (cm^{-1})	19500	13500	-	9800	4200

Table 3: Details of the components of the DMS surface's total number of points and fitting root-mean-squared-deviation (RMSD).

Interaction	H_3O^+	$H_3O^+Cl^-$	$H_3O^+H_2O$
Total Points	1601	11307	48189
$RMSD_x$ (a.u.)	0.0011	0.0061	0.0159
$RMSD_y$ (a.u.)	0.0024	0.0017	0.0106
$RMSD_z$ (a.u.)	0.0017	0.0014	0.0100

Table 4: MP2/aVDZ full harmonic frequencies (cm^{-1}) and intensities (km/mol) for the SIP configuration.

Frequency	Intensity
68	6
68	6
103	3
187	12
187	12
252	39
302	16
302	15
328	13
328	180
329	185
392	7
459	136
473	50
473	50
725	106
725	106
798	0
840	2
979	83
979	83
1489	463
1626	25
1626	25
1635	0
1758	29
1758	29
2649	1295
2650	1293
2880	979
3266	1072
3266	1070
3331	1242
3862	150
3862	151
3864	23

Table 5: Properties of the embedded H_3O^+ in the SIP configuration. Distances are reported in Ångstroms and angles in degrees.

	LMon PES	CCSD(T)-F12/aVDZ
OH-Bonds	1.018	1.020
Hydrogen-Bonds	1.550	1.538
Umbrella Angle	105.0	104.1
O$\cdots$Cl	3.541	3.535

Table 6: Summary of the SIP H_3O^+ harmonic stretch frequencies (cm^{-1}).

Theory	$\nu_{\text{Asym. Str.}}$	$\nu_{\text{Asym. Str.}}$	$\nu_{\text{Sym. Str.}}$
B3LYP/D9511(p,d) (S*4*)	2600	2608	2786
MP2/6-311+G* (S*5*)	2747	2747	2987
BLYP/aVTZ (S*6*)	-	-	2708
MP2/6-311+(3df,3pd) (S*7*)	-	-	2921
RI-MP2/aVTZ (S*8*)	-	-	2903
MP2/aVDZ	2649	2649	2880
CCSD(T)-F12/aVDZ (LMon)	2713	2713	2960
PES (LMon)	2803	2803	2957

Table 7: Results of weighted virtual state analysis for the twelve-mode H_3O^+ in the SIP configuration four-mode coupled spectra. Each band is labeled along with the number of IR active VCI states in the band. All states whose weighted coefficients are within 50% of the largest state's coefficient are shown for each respective bands. The percent of the largest virtual VSCF state are given, followed by the respective state. The twelve integers listed in each virtual VSCF state are the excitations from the ground state where each sequential number refers to respective harmonic mode.

---

5 States in 1300.0 - 1400.0
100.0 < 0 0 0 0 0 0 0 1 0 0 0 0 0 0 >

---

13 States in 2150.0 - 2220.0
100.0 < 0 0 0 0 0 1 0 1 0 0 0 0 0 0 >
55.87 < 0 0 0 0 0 0 1 1 0 0 0 0 0 0 >

---

21 States in 2370.0 - 2415.0
100.0 < 4 0 0 0 0 0 0 1 0 0 0 0 0 0 >
82.36 < 0 0 0 0 0 0 0 0 0 0 0 1 0 0 >
71.03 < 0 0 0 0 0 0 0 0 0 0 0 0 1 0 >

---

19 States in 2415.0 - 2473.0
100.0 < 0 0 0 2 1 0 0 0 0 0 0 0 0 0 >
97.70 < 0 0 0 2 0 1 0 0 0 0 0 0 0 0 >
64.67 < 1 0 1 0 2 0 0 0 0 0 0 0 0 0 >
64.13 < 1 1 0 0 1 1 0 0 0 0 0 0 0 0 >
62.69 < 1 1 3 0 0 1 0 0 0 0 0 0 0 0 >
60.63 < 1 0 1 0 0 2 0 0 0 0 0 0 0 0 >
58.91 < 0 1 1 0 0 2 0 0 0 0 0 0 0 0 >
51.52 < 0 1 1 0 2 0 0 0 0 0 0 0 0 0 >
50.66 < 1 1 3 0 1 0 0 0 0 0 0 0 0 0 >

---

15 States in 2480.0 - 2515.0
100.0 < 0 1 0 0 0 1 1 0 0 0 0 0 0 0 >
99.68 < 0 1 0 0 1 0 1 0 0 0 0 0 0 0 >
93.88 < 1 0 0 0 1 0 1 0 0 0 0 0 0 0 >
87.29 < 1 0 0 0 0 1 1 0 0 0 0 0 0 0 >
67.88 < 0 1 0 1 0 0 1 0 0 0 0 0 0 0 >
58.06 < 1 0 0 1 0 0 1 0 0 0 0 0 0 0 >
52.19 < 0 0 0 1 0 0 0 0 1 0 0 0 0 0 >

---

24 States in 2515.0 - 2560.0
100.0 < 0 0 0 0 0 0 0 2 0 0 0 0 0 0 >
84.20 < 0 0 0 0 0 0 0 0 0 0 0 0 0 1 >

---

50 States in 2680.0 - 2750.0
100.0 < 0 0 0 0 0 1 0 1 0 0 0 0 0 0 >
94.71 < 0 0 0 1 0 0 0 1 0 0 0 0 0 0 >
92.52 < 0 0 0 0 1 0 0 0 1 0 0 0 0 0 >
81.71 < 1 2 0 0 1 1 0 0 0 0 0 0 0 0 >
77.29 < 0 1 2 0 0 0 0 1 0 0 0 0 0 0 >
70.26 < 4 0 2 0 0 1 0 0 0 0 0 0 0 0 >
51.14 < 0 0 0 0 1 0 0 1 0 0 0 0 0 0 >

---

76 States in 2750.0 - 2860.0
100.0 < 0 0 0 0 0 0 0 0 0 0 0 0 0 1 >
70.05 < 1 0 0 2 1 0 0 0 0 0 0 0 0 0 >
53.89 < 0 4 0 0 0 0 0 1 0 0 0 0 0 0 >
53.73 < 0 1 0 2 0 1 0 0 0 0 0 0 0 0 >
50.18 < 0 0 0 0 0 0 0 2 0 0 0 0 0 0 >

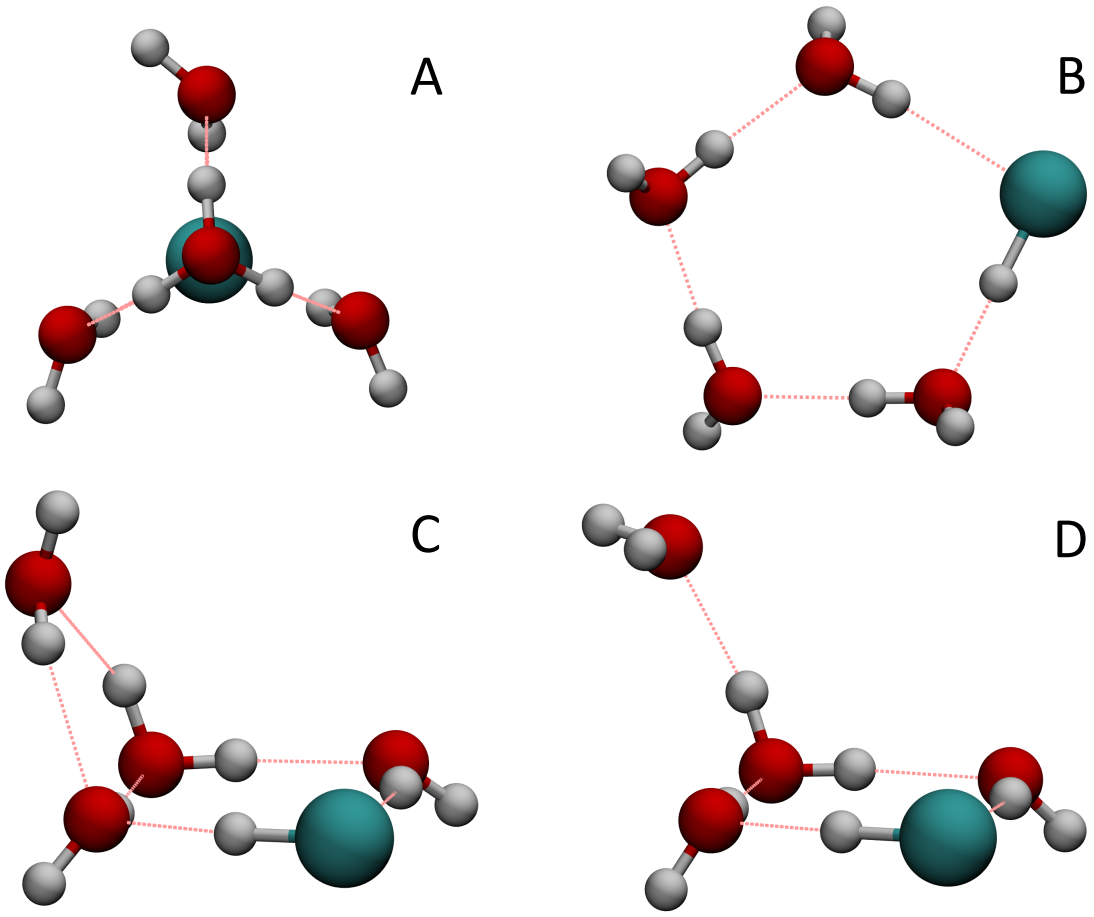

Figure 1: Higher energy local minima of the SIP and unionized $HCl(H_2O)_4$ cluster: (A), non-symmetric higher energy SIP cluster; (B), five-membered ring configuration; (C), four-member ring with water monomer accepting and donating a hydrogen bond to the ring; and (D) four-member ring with water monomer accepting a hydrogen bond from the ring.

Table 8: MP2/aVDZ full harmonic frequencies (cm^{-1}) and intensities (km/mol) for the SIP cluster in the alternate C_1 symmetry conformation.

Frequency	Intensity
70	9
77	2
103	3
180	10
192	16
251	38
273	74
294	28
310	51
326	110
337	141
393	11
430	33
469	82
518	134
671	92
723	67
807	27
819	43
960	98
1008	42
1482	453
1613	32
1625	18
1645	7
1740	26
1771	39
2622	1340
2692	1247
2891	966
3253	1144
3285	1011
3341	1211
3862	124
3868	65
3869	132

Table 9: CCSD(T)-F12/aVDZ local harmonic frequencies (cm^{-1}) for the SIP cluster in the alternate non-symmetric conformation.

Frequency
221
243
305
769
873
922
1470
1763
1793
2683
2757
2969